THERMALHYDRAULIC RESPONSE OF A CONCEPTUAL CANDU REACTOR WITH A HIGHLY ADVANCED CORE SUBJECT TO VARIOUS LOSS-OF-COOLANT ACCIDENTS

J. Vecchiarelli, R.F. Dam, K.F. Hau, and F.J. Doria

Atomic Energy of Canada Limited
2251 Speakman Drive
Mississauga, Ontario
Canada L5K 1B2

ABSTRACT

Thermalhydraulic simulations of a conceptual CANDU plant with a highly advanced core (HAC) have been conducted for various loss-of-coolant accident (LOCA) scenarios. A distinctive feature of the HAC core is the lack of a power pulse due to zero void-reactivity. In the present study, the following LOCA cases were investigated: a 100% reactor outlet header break and reactor inlet header breaks ranging in size from 5% to 25%. A SOPHT circuit model was employed to predict the system response during the initial high-pressure stage of emergency core coolant (ECC) injection. Only one ECC train was assumed to be operable. The investigation focused on core flow characteristics, in particular, stagnation conditions in the critical pass. Other aspects of interest include void distributions and depressurization rates of the heat transport system. Detailed fuel-element analyses were also performed to estimate maximum sheath temperatures, based on header boundary conditions from the SOPHT simulations.

1. Introduction

A design study of a conceptual CANDU-type reactor featuring a Highly Advanced Core (HAC) has been completed for the Electric Power Development Company (EPDC) of Japan. The HAC CANDU reactor has 640 fuel channels, and it produces 3990 MWt at full power (the net electrical output of the plant is roughly 1300 MWe). Twelve fuel bundles are enclosed within each channel. The bundles are comprised of 61 fuel elements arranged in five concentric rings. The outer three rings contain slightly enriched uranium-235 (about 3%), while the inner two rings contain depleted uranium-235 and dysprosium. The amount of dysprosium is such that the reactor core has essentially zero void-reactivity.

This paper highlights the results from thermalhydraulic analyses [1] in which the conceptual HAC CANDU reactor was subjected to various loss-of-coolant accident (LOCA) scenarios. Specifically, the following cases were investigated: a 100% reactor outlet header (ROH) break and reactor inlet header (RIH) breaks ranging in size from 5% to 25%. The SOPHT code (version SOPHT-HAC-XX.HP1.1.1) was employed to simulate the thermalhydraulic behaviour of the reactor circuit, including the primary heat transport (HT) system, the emergency core coolant (ECC) system[1], and the auxiliary system components. Figure 1 displays the nodalization associated with the SOPHT circuit model (ECC system model not shown). In this model, a simplified treatment of the HAC core is used; the 640 fuel channels are represented by four core passes.

The transient header conditions and reactor power from the SOPHT simulations were input to a CATHENA model [1] of a single high-power fuel channel. Based on the computed results from the CATHENA simulations, detailed fuel-element analyses were subsequently performed using ELESTRES and ELOCA models [1].

2. Main Assumptions For SOPHT Circuit Analyses

The main assumptions in the SOPHT circuit analyses for the RIH and ROH LOCA cases are listed as follows.

1. The computed break-discharge flow rate is based on the Henry-Fauske model, except when the void fraction in a broken header is identically zero, in which case the orifice model is used.

2. The primary reactor trip signals (including instrumentation delays) are: low coolant flow rate, low ROH pressure, low differential pressure across RIH and ROH, and high containment pressure.

---

[1]Only the high-pressure portion of the ECC system was modelled.

3. Loss of class IV power is assumed immediately upon reactor trip.

4. The LOCA signal is a low ROH pressure coupled with a high containment pressure signal; the latter signal is assumed to occur earlier than the former.

5. Loop isolation is initiated on a LOCA signal.

6. Crash cooling of the steam generators is credited after the LOCA signal, and the number of main steam safety valves (MSSVs) credited is assumed to be 3 out of 4 (that is, a total of 12 MSSVs).

7. Only one of the two ECC trains are assumed to be operational.

3. SOPHT Circuit Analyses For RIH LOCAs

3.1 Case Descriptions

The following scenario is considered for a general RIH LOCA. The reactor is initially operating at a steady–state condition corresponding to 102% full power (4070 MWt). At time zero, a RIH break occurs. The break is specified to occur at RIH 4; for the same break area and initial conditions, it is assumed that the differences in the overall transients for breaks at other RIH locations is relatively small. In the present study, RIH break sizes ranging from 5% to 25% were considered. This range includes cases in which the critical core pass (that is, from RIH 4 to ROH 1) experiences reverse flow, positive flow, and sustained stagnation conditions. For each case considered, Table 1 gives a summary of pertinent details, such as the timing of various control actions.

3.2 Analysis Results For 25% RIH LOCA

Overall, the discharge flow rate from the broken header (RIH 4) tends to decrease as time increases; the flow depends on both the header pressure and quality, which vary during the transient. The maximum discharge flow rate occurs at the instant of the break and is approximately 8670 kg/s.

Due to the break discharge flow, the broken header rapidly depresssurizes, as shown in Figure 2. The other three headers in the broken loop also depressurize. The initial depressurization rate is largest for the broken header. The headers in the intact loop depressurize slowly, compared with header pressures in the broken loop.

The reduction in header pressures results in a decrease of the header-to-header pressure drop across each core pass (this is evident in Figure 2). Consequently, the flow through each pass initially decreases. The reactor trips shortly (at 0.25 s) after the flow through the critical pass reaches the low flow set point.

At the time of the trip, the reactor power begins to decrease and a loss of class IV power is assumed to occur. The latter incident causes the four HT pumps to run down, which contributes to further depressurization of the HT system. In addition, the feedwater to the steam generators and the steam flow to the turbines are completely cut off after the trip. As a result, the pressure in the steam generators initially builds up because heat from the HT system continues to be transferred.

As the HT system gradually depressurizes, a LOCA signal is detected at 9.66 s due to the pressure in ROH 1 dropping below the set point. At the time of the LOCA signal, the ECC gas valves and high pressure isolation valves are simultaneously opened. At 11.16 s (1.5 s after the LOCA signal), the MSSVs are opened in order to crash cool the steam generators, the loop isolation valves begin to close, and the ECC injection valves begin to open. When the HT system pressure is below the ECC system pressure, ECC injection takes place. Figure 3 shows the ECC injection flow rate for all headers. It is noted that ECC injection into the broken header is restricted in the present study. For the simulation time considered, only the broken loop receives ECC. Moreover, the ECC injection occurs in the following order: ROH 1, ROH 3, and RIH 2. This sequence is consistent with the header pressure transients which are shown in Figure 2, where it is observed that near the time of the LOCA signal the ROH 1 pressure is less than the ROH 3 pressure, which is less than the RIH 2 pressure.

Figure 3 indicates that the ECC flows briefly surge at about 23 s. This is attributed to header pressure spikes that occur near the same time, as observed in Figure 2. These pressure spikes are a consequence of a void collapse in ROH 1, as evidenced in Figure 4. The void collapse is attributed to ECC injection. The void collapse in ROH 1 is followed immediately by pressure spikes. It is noted that the magnitude of the pressure spikes may be exaggerated because of numerical effects; however, the existence of these pressure spikes is physically justifiable.

Figure 5 shows the variation of the flow rate through the center of each core pass. Except in the critical core pass (4–1), the flows are predominantly in the forward direction. For the critical pass, a considerable reverse flow is established. Basically, the break in RIH 4 is large enough that the pressure in RIH 4 falls below the pressure in ROH 1, as seen in Figure 2. During the transient, the negative header-to-header pressure drop across the critical pass is sustained. The magnitude of the reverse flow is largest in the initial phase of the transient. It is significantly smaller from about 15 to 30 s, but is then re–established after 30 s due to the ECC injection.

Figure 6 shows the void fraction at the center of each core pass. During most of the simulation time, there is significant void in the critical pass. However, the void begins to disappear in the final stages of the transient, as the ECC injection causes the reverse flow to increase.

Following the RIH break and prior to the reactor trip, the reactor power is constant. A power pulse is not exhibited because of the zero void-reactivity of the HAC core. After the trip has occurred, the power monotonically decreases as time increases.

3.3 Analysis Results For 10% RIH LOCA

The predicted transients of the reactor power, break discharge flow, header pressures, HT pump speed transients, ECC injection flows, boiler pressures, pressurizer level, and gas tank and water tank pressures are qualitatively similar to the results obtained for the 25% case. That is, the trends in the variations of these quantities are similar for the 10% and 25% RIH break cases.

For the 10% RIH break, the maximum break discharge flow rate is 3470 kg/s. The reactor trips at 0.44 s (due to low coolant flow rate), which is later than the trip time for the 25% case, as expected since the 10% break size results in a less rapid reduction of the coolant flow. The LOCA signal for the 10% RIH break is detected at 18.44 s, which is also later than the timing of the LOCA signal for the 25% case (since the rate of HT system depressurization with the latter break size is greater than that of the former).

Figure 7 suggests that the 10% RIH break size results in sustained stagnation conditions in the critical pass. The duration of the stagnation conditions is from approximately 18 to 73 s; the temporary surges in flow through the pass are attributable to changes in ECC injection flow, which are caused by header pressure spikes due to void collapses in the headers. A considerable reverse flow in the critical pass is established after 73 s; this reverse flow is caused by ECC injection. It is noted that near stagnation conditions exist between approximately 2 and 8 s, during which time the reactor power is relatively large, in comparison to the power during the period of sustained stagnation conditions.

Figure 8 shows the predicted void fraction at the center of the core passes. It is observed that, during most of the transient, the void fraction is relatively large in the critical pass. Just after 76 s, when reverse flow has started in this pass, the void fraction begins to decrease as time progresses. At roughly 98 s, the void in the center of the critical pass vanishes.

3.4 Analysis Results For 5% RIH LOCA

The predicted transients of the reactor power, break discharge flow, broken-loop header pressures (Figure 9), intact-loop header pressures, ECC injection flows, HT pump speed transients, boiler pressures, pressurizer level, and gas tank and water tank pressures are qualitatively similar to the results obtained for the 10% case.

For the 5% RIH LOCA, the maximum break discharge flow rate is 1730 kg/s. The reactor trips at 2.75 s (due to low coolant flow rate), which is significantly later than the trip time for the 10% case. The reason for the large increase in trip time is explained as follows. The reactor trip time depends heavily on the rate of depressurization of the broken RIH. The depressurization rate is a function of the break size. As the break size approaches zero (no LOCA), the trip time approaches infinity. Thus, a small decrease in the break size results in a large increase in the reactor trip time, at relatively small break sizes. This trend is evident in Table 1; the trip time increases significantly as the RIH break size decreases from 8% to 5%. In contrast, the trip time is much less sensitive to break sizes which are relatively large, as seen in the trip times for 25% and 10% RIH break sizes in Table 1. The core coolant flow rate reduces less rapidly in the 5% case than it does in the 10% case. The LOCA signal for the 5% RIH break is detected at 29.93 s, which is also later than the timing of the LOCA signal for the 10% case (because the rate of HT system depressurization with the latter break size is greater than that of the former).

Figure 10 shows that the 5% break case has a stronger tendency for forward flow in the critical pass than does the 10% break case. The flow slows down after 40 s due to the large void fraction in the critical pass at that time (see Figure 11). However, the flow increases again as the void reduces after 50 s because of the ECC injection. Later, as the void increases, the flow again slows. Unlike in the 10% case, the 5% RIH break does not produce near stagnation conditions in the critical pass during the initial phase of the transient. Instead, the initial flow in all core passes remains in the forward direction.

From inspection of Figures 9 and 10, it is noticed that forward flow persists in the critical pass for over 40 s, even though the pressure in ROH 1 exceeds the pressure in RIH 4 during the time period of 15 to 40 s. The reason for the forward flow is explained as follows. Firstly, the elevation drop between RIH 4 and the inlet of core pass 4–1 is approximately the same as the elevation rise between the outlet of core pass 4–1 and ROH 1. Secondly, the density of the fluid in the inlet feeders is considerably larger than the fluid density in the outlet feeders. As a result, the integrated gravitational pressure is greater at the inlet of the critical pass than at the outlet. Moreover, it was confirmed that the sum of the header pressure and the feeder integrated gravitational pressure is greater at the inlet of the critical pass than at the outlet. Hence, the fluid flows from RIH 4 to ROH 1, even though the pressure in the latter is greater than the pressure in the former. Thus, it is concluded that the direction of flow in the critical core pass is physically correct, for the time period in question.

4. SOPHT Circuit Analysis For 100% ROH LOCA

4.1 Case Description

The following scenario is considered for the 100% ROH LOCA case. The reactor is initially operating at a steady–state condition corresponding to 102% full power. At time zero, a 100% ROH break occurs. The break is specified to occur at ROH 3. It is thought that this represents a worst-case scenario, based on the premise that a break in a ROH which is not connected to the pressurizer is less severe than a break in a ROH connected to the pressurizer. The rationale is that the pressurizer aids in driving water through the critical pass for the former, whereas for the latter, the pressurizer flow goes to the break.

4.2 Analysis Results

Table 2 provides a summary of the key parameters of the circuit analysis for the 100% ROH LOCA case.

The relatively large discharge flow causes the broken header (ROH 3) to have a rapid pressure drop over the first second of the transient (see Figure 12). As expected, the downstream inlet header (RIH 4) follows the pressure drop of ROH 3 with only a slight delay caused by inertia effects. The upstream inlet header (RIH 2) continues to receive flow from ROH 1 and consequently shows a significantly slower pressure decline. ROH 1 is furthest from the break location, and it shows the slowest response to the break of the headers in the broken loop.

The pressure changes in the headers affect the inlet feeder flows as follows. The flow from RIH 2 to ROH 3 initially increases in response to the increased pressure drop produced by the rapidly reducing pressure in ROH 3. Conversely, the flow from RIH 4 to ROH 1 reduces quickly as the RIH 4 pressure reduces and decreases the pressure drop in this core pass. Before the reactor trip, there is no noticeable change in the flows through the intact loop.

At 0.9 s the low header pressure trip signal is received, and the reactor power begins to decrease. The HAC core does not develop a power pulse because of the zero void-reactivity. There is no change in power leading up to the time of the trip. After the trip, the power reduces rapidly.

At the time of the trip, there is an assumed loss of class IV power, which results in loss of the pressurizer heaters and the loss of all HT pumps. The pumps continue run down during the duration of the transient. Pump 2 is eventually stopped by reverse flow, whereas the higher flow seen through pump 1 results in the pump continuing to run down throughout the simulation.

The feedwater to the steam generators and the steam flow to the turbines are cut off at the time of the trip (0.9 s) in 0.1 s. This results in an initial pressurization of the boilers since energy from the HT system continues to be transferred to the steam generators. This reduces the ability of the steam generators to remove energy from the HT system.

At 1.36 s the low pressure signal for the LOCA is detected. This signal, in conjunction with the conditional signal of high containment pressure (which is assumed to occur at 1.0 s), results in a LOCA signal at 1.36 s. At this time the ECC gas valves and high pressure isolation valves are opened. This primes the ECC system for injection.

After the LOCA signal, the broken header pressure continues to fall, although it is slowing somewhat with the reduction in break discharge flow rate. The break discharge significantly reduces when the void fraction of the fluid leaving the break increases significantly. As the transient progresses, the break discharge follows the system pressure transient.

The flow in the intact pass of the broken loop begins to reverse as the RIH 4 pressure falls below the ROH 1 pressure, reaching a peak reverse flow at approximately 1.8 s. There is significant flow reversal predicted for the HAC design, which is attributed to the high fluid inertia in the HT system. The intact pass flow then recovers and reaches a near stagnant condition in the inlet feeder shortly after 5 s. The RIH 4 pressure adjusts to approximately equal the ROH 1 pressure, which produces the stagnation condition. The stagnant condition results in a significant increase of the void fraction in the core pass (see Figures 13 and 14). The stagnation location is expected to move within the channel as header conditions continue to change. The flow in the center of the channel is predicted to stagnate for approximately 4 s, whereas the flow in the inlet feeder completely stagnates only momentarily.

While the pressures continue to fall in the broken loop, and before the stagnation conditions begin to appear, the ECC injection valves start to open at 2.86 s. However, the ECC system pressure remains below the HT system pressure until approximately 6 s, which prevents any ECC injection until that time. The pressure in RIH 4 and ROH 1 reach the ECC system pressure first and injection begins at these locations almost simultaneously. The pressure in RIH 2 matches the ECC system pressure 2 s later, resulting in a delay in ECC injection to that header.

At 2.86 s the MSSVs also open to crash cool the steam generators. The impact on the broken loop pressure transient is minimal since the break is the dominating cause of the pressure drop in the HT system. In the intact loop, the crash cool is the only means of pressure reduction since the feedwater is cut off at the time of the reactor trip. The steam generator pressures decrease following the crash cool. The steam generators are not isolated from each other during the transient, and therefore the boiler pressures tend to remain equal.

The ROH 1 void collapses at 12.7 s, as the ECC system begins to refill the HT system. Incidentally, the ECC injection valves are fully open by 12.86 s. The injection rate continues to increase until approximately 25 s. During this time the void is being collapsed in the channel, as seen by the reduction in the channel void at the center (Figure 14). The maximum ECC injection flow rates are in the range of 600 to 800 kg/s.

For the remainder of the transient, the break discharge rate drops as the HT system pressure drops in the broken loop. The broken-loop pressure falls below 2 MPa by 50 s. The ECC system pressure also drops, but remains above 4 MPa at 50 s. After 30 s, void collapse is occurring around the broken loop as refill begins, resulting in pressure variations in the headers.

5. Fuel-Element Analyses

Based on computed data from the SOPHT circuit analyses, fuel-element analyses were conducted to estimate fuel and sheath temperatures during each LOCA transient. The SOPHT time-dependent header conditions corresponding to the critical core pass were used as boundary conditions in a CATHENA model of a single high-power HAC fuel channel. The predicted reactor power transient was also input to the CATHENA model. Certain thermalhydraulic results from the CATHENA analysis were subsequently specified as boundary conditions in detailed ELESTRES (steady-state) and ELOCA (transient) models of the HAC fuel elements in the particular high-power channel.

Sample computed results from the fuel-element analyses are displayed in Figure 15. It is interesting to point out that the maximum sheath temperature for the 15% RIH break is practically the same as that for the 10% RIH break. In the latter case, the maximum sheath temperature is attained during a period when there is sustained stagnation of channel flow at relatively low reactor power. In the former case, the maximum sheath temperature occurs very early in the transient, when the reactor power is relatively high and the channel flow stagnates momentarily before significant reversal.

With respect to the 100% ROH LOCA case, the predicted maximum sheath temperature is 802°C; a higher temperature may develop with a smaller ROH break size. For all of the LOCA cases which were examined, the fuel-element analysis results satisfy the EPDC acceptance criterion that the maximum sheath temperature shall remain below 1200°C.

6. Conclusions

The SOPHT results from the present RIH and ROH LOCA assessment of the conceptual HAC CANDU reactor suggest that a 10% RIH LOCA and a 100% ROH LOCA cause sustained stagnation conditions in the critical core pass. A significant reverse flow in this core pass is established with larger RIH breaks, while all core flows are predominantly positive with smaller RIH breaks. Subsequent fuel-element analyses using CATHENA, ELESTRES, and ELOCA indicate that the 10% and 15% RIH LOCAs lead to the highest sheath temperatures. The qualitative trends observed in this study provide insight on the thermalhydraulic behaviour of CANDU-type reactors.

Acknowledgements

The authors acknowledge the financial contribution of EPDC and thank EPDC for permission to disseminate data from analyses of the HAC design.

References

1. Dam, R.F., Doria, F.J., Hau, K., and Vecchiarelli, J., "ROH and RIH LOCA Assessment", Task 18.2, EPDC FY 1996 Conceptual Design Study of the Highly Advanced Core (HAC) CANDU System, 35-33100-CDS-9613, Final, March 1997.

Table 1 Summary Of SOPHT Results For Various HAC CANDU RIH LOCA Cases

	5% RIH Break	8% RIH Break	10% RIH Break	15% RIH Break	25% RIH Break
Area of break (m^2)	0.02027	0.03243	0.04054	0.06080	0.1013
Maximum Break Discharge Flow (kg/s)	1730	2780	3470	5200	8670
Reactor Trip Time (s)	2.75	0.60	0.44	0.32	0.25
LOCA Signal (s)	29.93	20.47	18.44	14.13	9.66
Initiation Of ECC Injection Valves, Isolation Valves, and MSSVs (s)	31.43	21.97	19.94	15.63	11.16
ECC Injection: First Injection (s)	35.8	25.0	23.3	16.5	12.7

Note: break occurs at time zero

Table 2 Summary Of SOPHT Results For HAC CANDU 100% ROH LOCA

	HAC
LOCA Signal	1.36 s
Trip time	0.9 s on low ROH pressure
Break Size	0.4215 m^2
Peak Break Discharge	20235 kg/s
ECC Injection: Valve Initiation	2.86 s
ECC Injection: First Injection	5.8 s

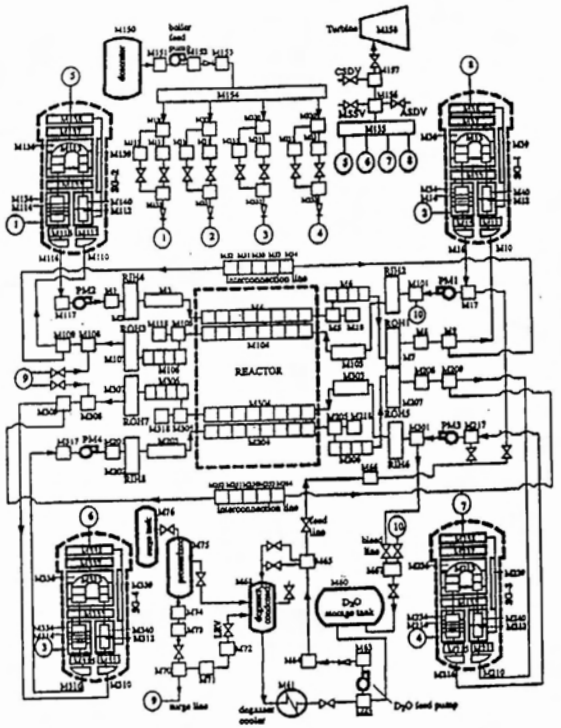


Figure 1 SOPHT four-quadrant model of HAC CANDU.

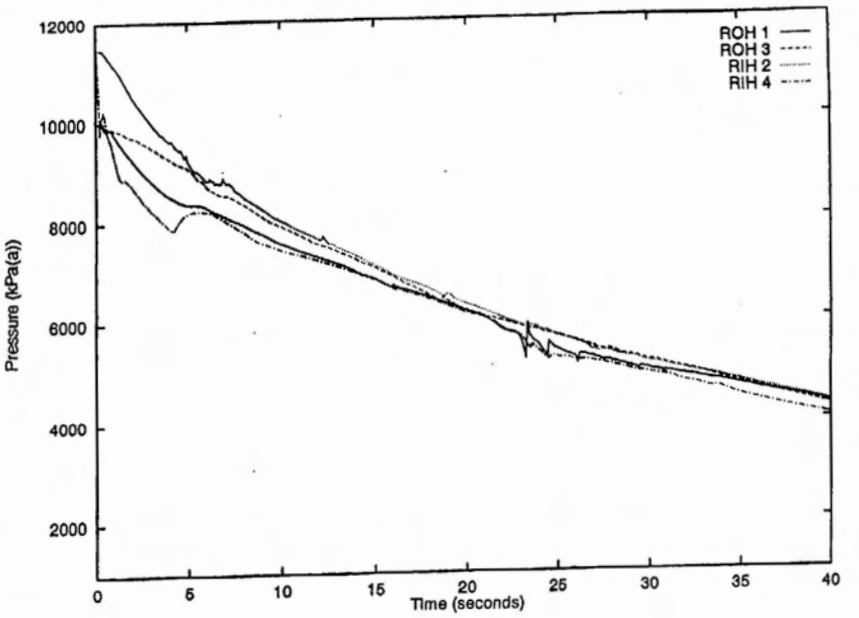


Figure 2 SOPHT pressure transients in broken loop of HAC CANDU, for 25% RIH LOCA.

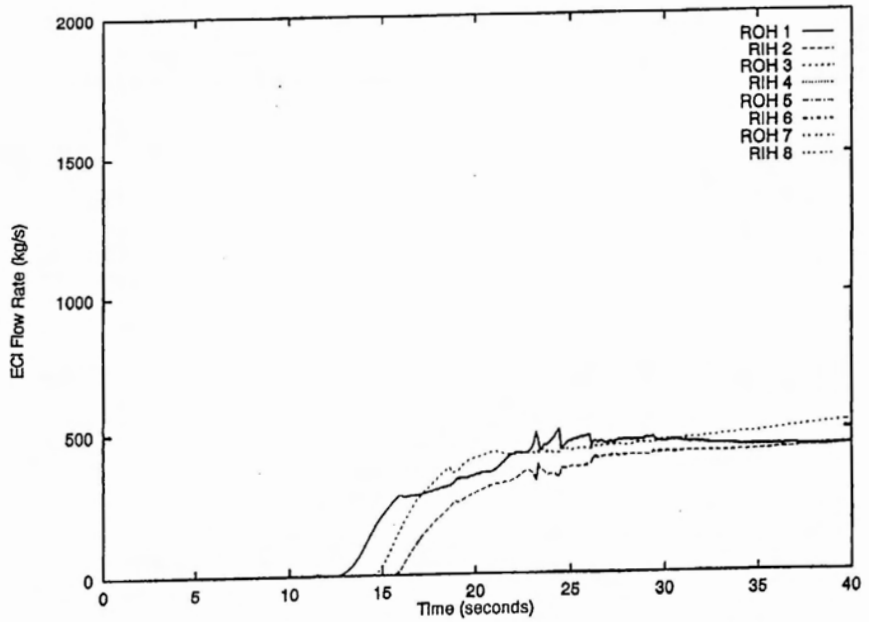


Figure 3 SOPHT ECC injection flow transients in HAC CANDU, for 25% RIH LOCA.

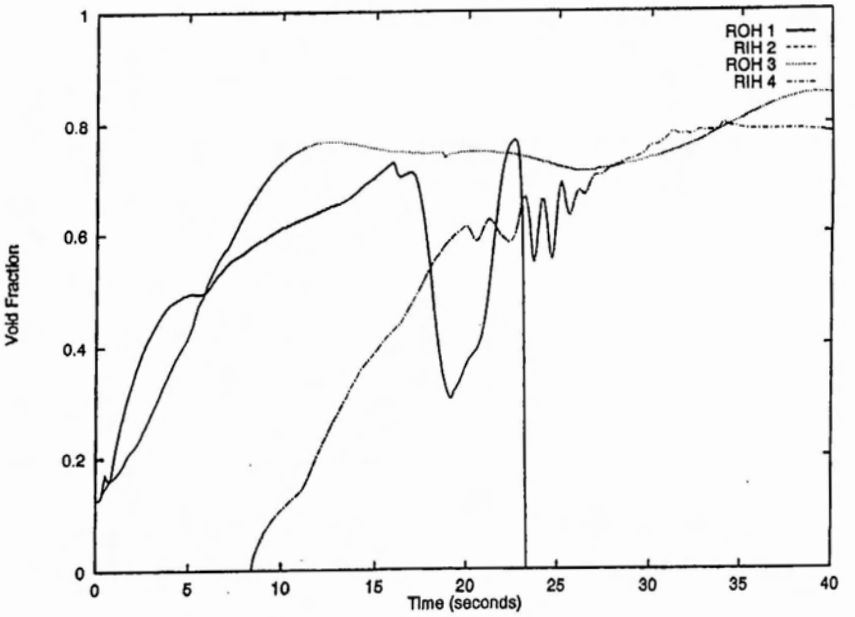


Figure 4 SOPHT header void-fractions in broken loop of HAC CANDU, for 25% RIH LOCA.

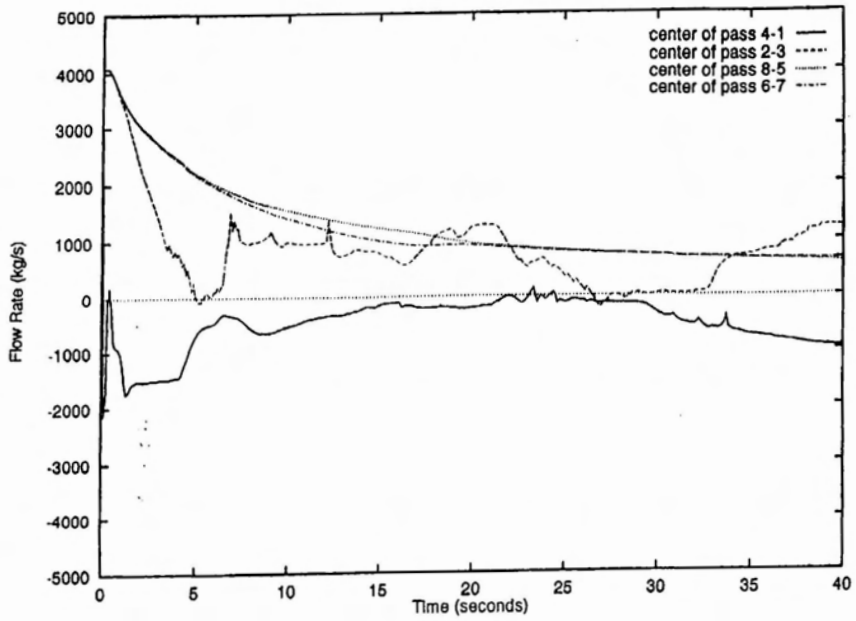


Figure 5 SOPHT flow transient in center of core passes of HAC CANDU, for 25% RIH LOCA.

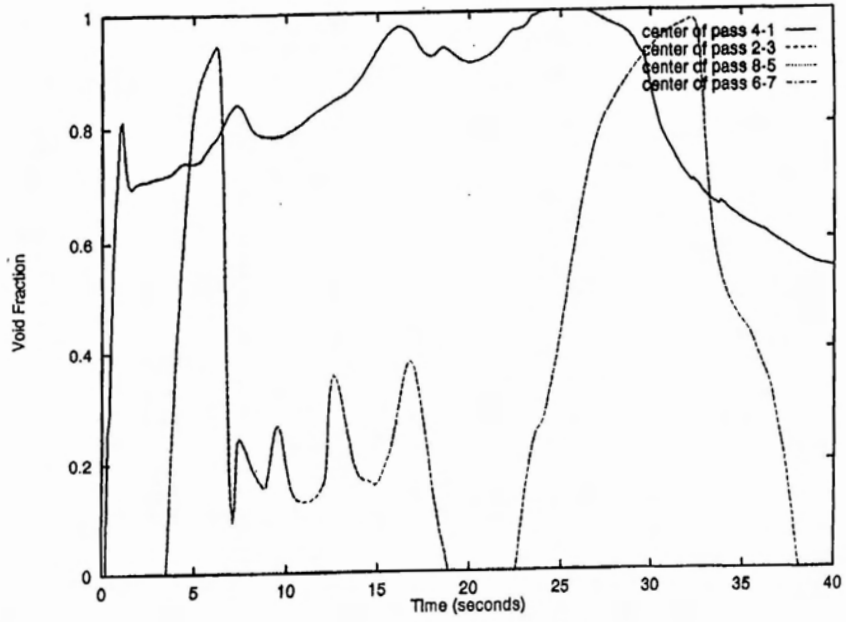


Figure 6 SOPHT void fraction in center of core passes of HAC CANDU, for 25% RIH LOCA.

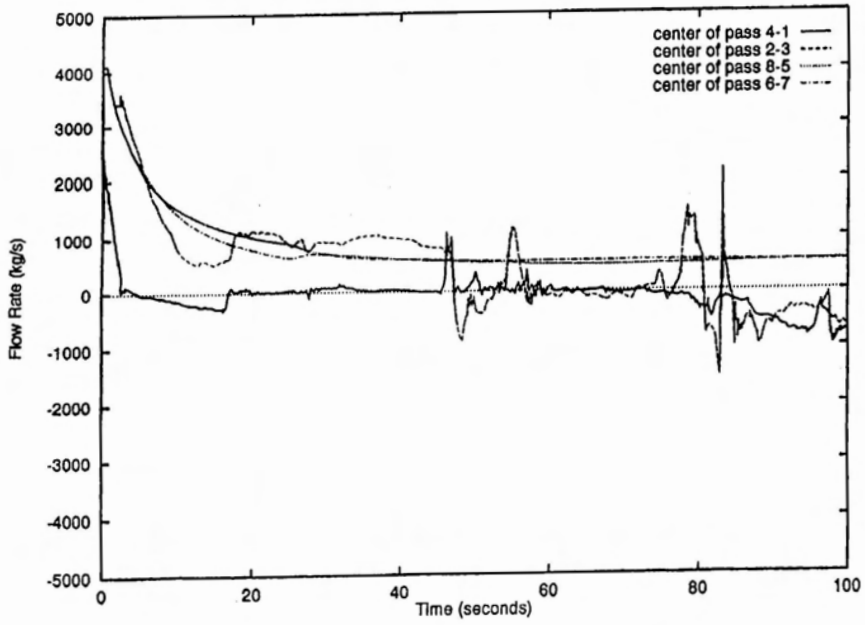


Figure 7 SOPHT flow transient in center of core passes of HAC CANDU, for 10% RIH LOCA.

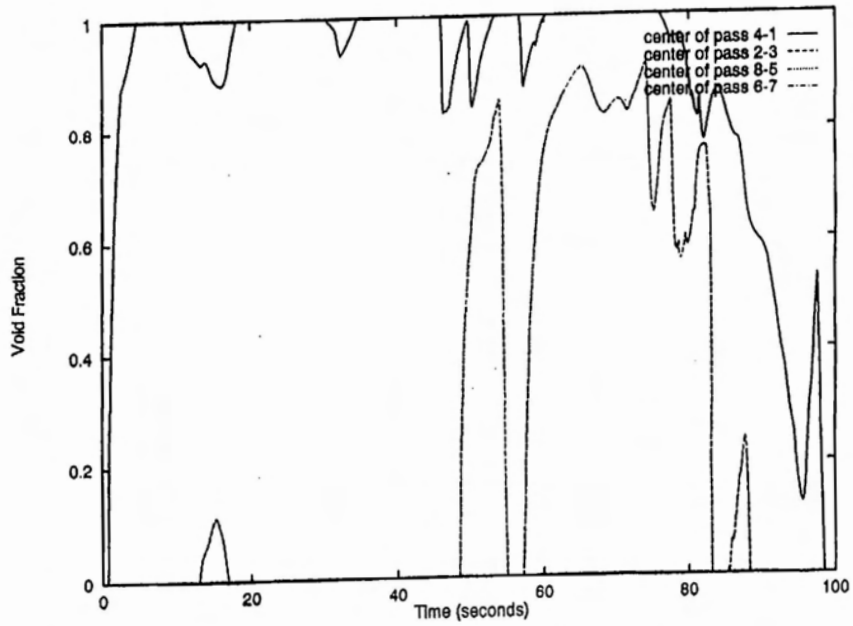


Figure 8 SOPHT void fraction in center of core passes of HAC CANDU, for 10% RIH LOCA.

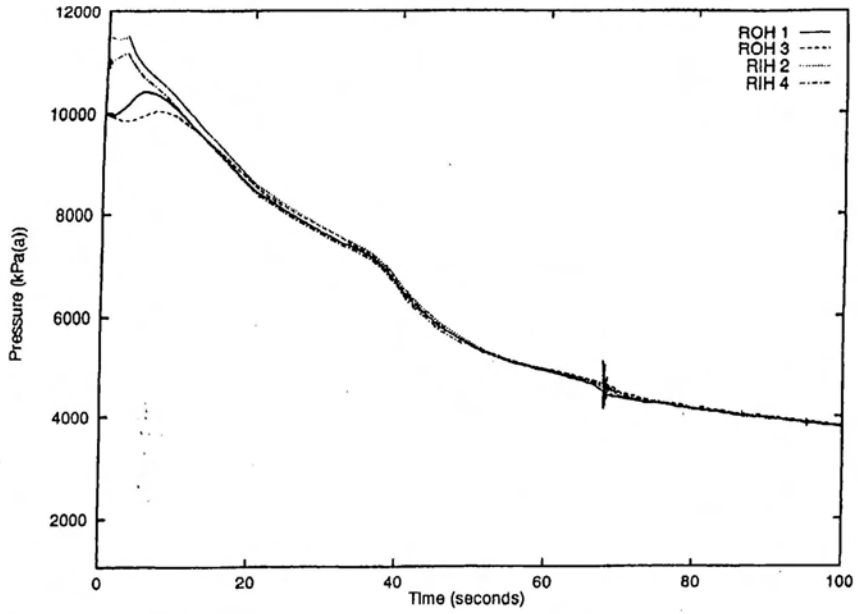


Figure 9 SOPHT pressure transients in broken loop of HAC CANDU, for 5% RIH LOCA.

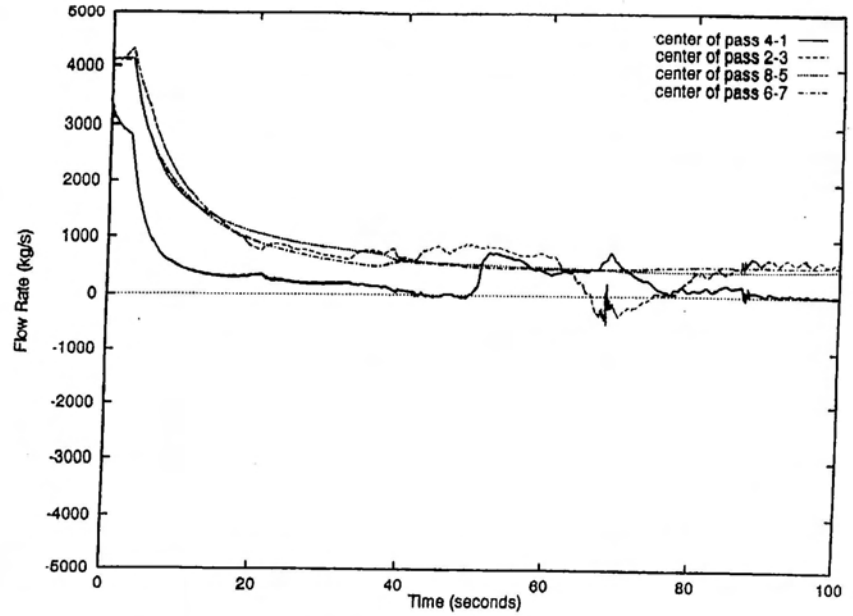


Figure 10 SOPHT flow transient in center of core passes of HAC CANDU, for 5% RIH LOCA.

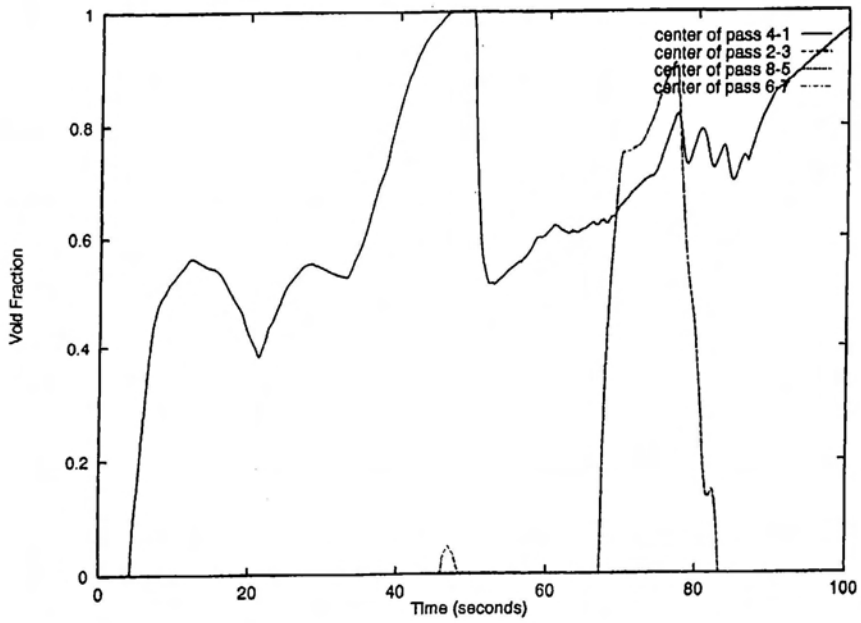


Figure 11 SOPHT void fraction in center of core passes of HAC CANDU, for 5% RIH LOCA.

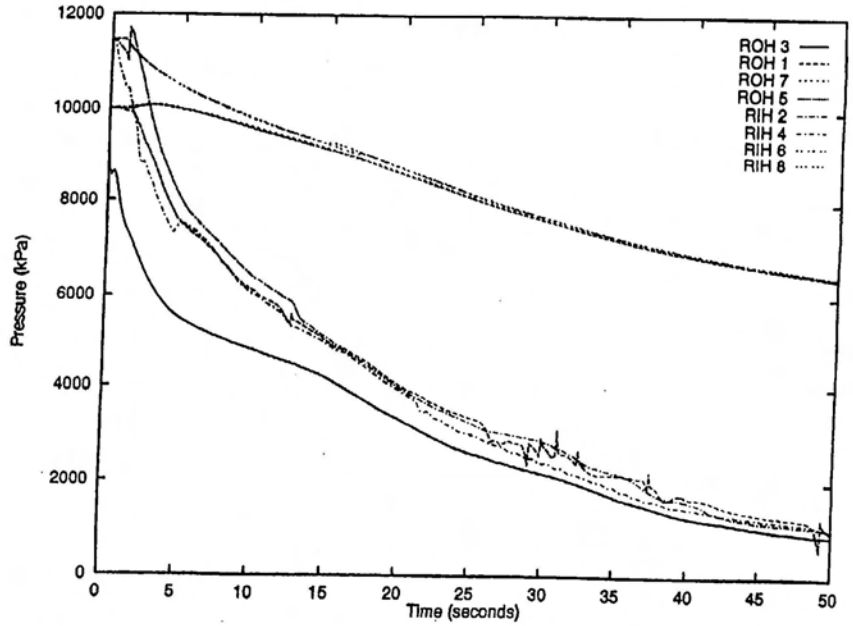


Figure 12 SOPHT pressure transients in HAC CANDU, for 100% ROH LOCA.

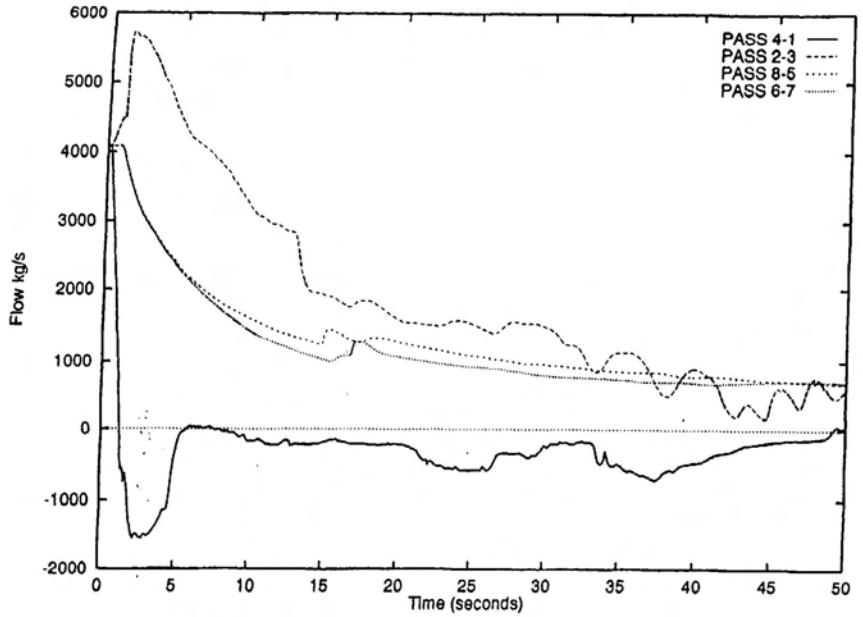


Figure 13 SOPHT flow transient in center of core passes of HAC CANDU, for 100% ROH LOCA.

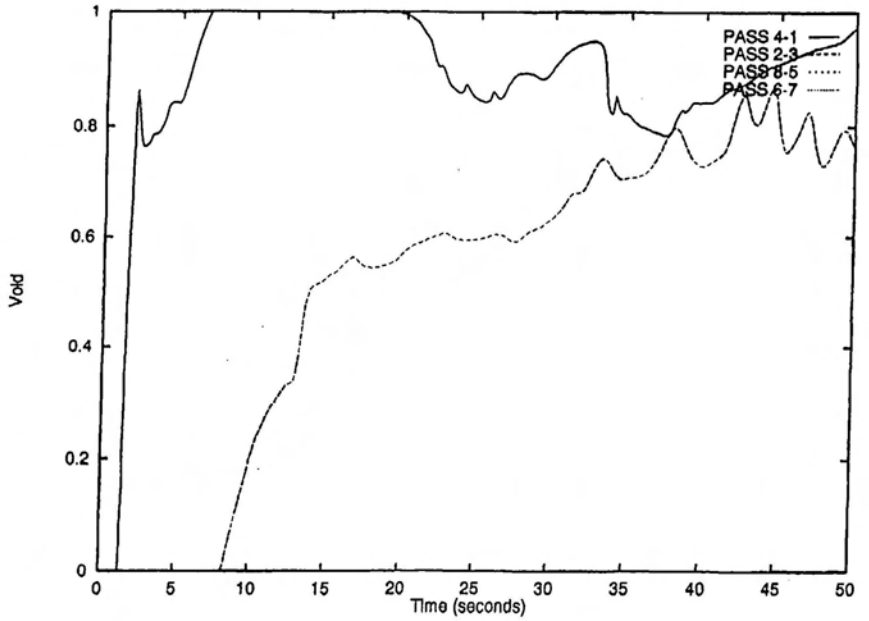


Figure 14 SOPHT void fraction in center of core passes of HAC CANDU, for 100% ROH LOCA.

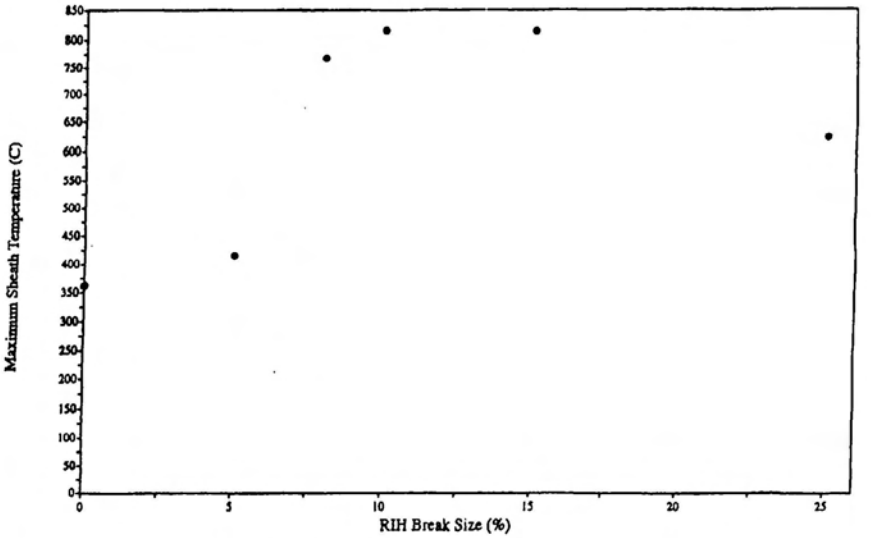


Figure 15 Maximum sheath temperature as a function of RIH break size, for HAC CANDU.